Mol Cell Biochem
DOI 10.1007/s11010-016-2784-0

Resistance to pathologic cardiac hypertrophy and reduced expression of $Ca_V1.2$ in Trpc3-depleted mice

Jung Woo Han[1] · Young Ho Lee[2] · Su-In Yoen[2] · Joel Abramowitz[3] · Lutz Birnbaumer[3] · Min Goo Lee[1] · Joo Young Kim[1]

Received: 27 April 2016 / Accepted: 5 August 2016

Abstract Sustained elevation of intracellular Ca^{2+} concentration ($[Ca^{2+}]_i$) reprograms cardiovascular cell fate, leading to cellular hypertrophy via Ca^{2+}-calmodulin/calcineurin (Cn)/NFAT activation. Accumulating evidence suggests that transient receptor potential canonical (Trpc) channels play important roles in the development of pathologic cardiac hypertrophy. Here, we demonstrated that Trpc3 mediates pathologic cardiac hypertrophy in neurohumoral elevation via direct regulation of $Ca_V1.2$ expressions. Elevated PE (phenylephrine) was maintained in mice by continuous infusion using an osmotic pump. Wild-type (WT) mice, but not *Trpc3*$^{-/-}$ showed a sudden decrease in blood pressure (BP) or death following elevation of BP under conditions of elevated PE. *Trpc3*$^{-/-}$ mesenteric artery showed decreased PE-stimulated vasoconstriction. Analysis of morphology, function, and pathologic marker expression revealed that PE elevation caused pathologic cardiac hypertrophy in WT mice, which was prevented by deletion of *Trpc3*. Interestingly, protection by *Trpc3* deletion seemed to be a result of reduced cardiac $Ca_V1.2$ expressions. Basal and PE induced increased expression of protein and mRNA of $Ca_V1.2$ was decreased in *Trpc3*$^{-/-}$ heart. Accordingly, altered expression of $Ca_V1.2$ was observed by knockdown or stimulation of *Trpc3* in cardiomyocytes. These findings suggest that Trpc3 is a mediator of pathologic cardiac hypertrophy not only through mediating part of the Ca^{2+} influx, but also through control of $Ca_V1.2$ expressions.

Keywords Transient receptor potential canonical channels 3 · L-type Ca^{2+} channel · Pathologic cardiac hypertrophy · Ca^{2+} influx

Abbreviations

$[Ca^{2+}]_i$	Intracellular calcium concentration
Trpc	Transient receptor potential canonical
BP	Blood pressure
PE	Phenylephrine
AngII	AngiotensinII

Electronic supplementary material The online version of this article (doi:10.1007/s11010-016-2784-0) contains supplementary material, which is available to authorized users.

✉ Joo Young Kim
jooyoungkim@yuhs.ac

Jung Woo Han
ad2011@naver.com

Young Ho Lee
YHLEE@yuhs.ac

Su-In Yoen
YSI2012@yuhs.ac

Joel Abramowitz
abramow1@niehs.nih.gov

Lutz Birnbaumer
birnbau1@gmail.com

Min Goo Lee
mlee@yuhs.ac

[1] Department of Pharmacology and Brain Korea, 21 PLUS Project for Medical Science, Yonsei University College of Medicine, 50 Yonsei-ro, Seodaemun-gu, Seoul 120-752, South Korea

[2] Department of Physiology and Brain Korea, 21 PLUS Project for Medical Science, Yonsei University College of Medicine, Seoul 120-752, South Korea

[3] Laboratory of Neurobiology, National Institute of Environmental Health Sciences, Research Triangle Park, Durham, NC 27709, USA

Published online: 13 August 2016

Cn/Ca^{2+}	Calmodulin-dependent protein phosphatase calcineurin
NFAT	Nuclear factor of activated T cells
ANF	Atrial natriuretic factor
BNP	Brain natriuretic peptide
β-MHC	B-myosin heavy chain
OAG	1-Oleoyl-2-acetyl-sn-glycerol

Introduction

Pathologic cardiac hypertrophy, or abnormal growth and remodeling of the heart, is caused by chronic pressure overload, massive tissue injury, or abnormal neurohumoral stimulation. It frequently results in heart failure, which is a leading cause of morbidity and mortality in developed countries [1, 2]. In this state, growth and protein synthesis of individual myocytes is hampered by excessive activation of multiple signaling pathways and alterations in gene expression [3]. Abnormalities in intracellular calcium concentration ($[Ca^{2+}]_i$) and Ca^{2+}-dependent signaling initiate and maintain pathologic cardiac hypertrophy through the Ca^{2+}/calmodulin-dependent protein phosphatase, calcineurin (Cn), which dephosphorylates the transcription factor nuclear factor of activated T cells (NFAT) [4]. Dephosphorylated, activated NFAT translocates into the nucleus, where it induces hypertrophic gene expression [5].

Trpc channels have been shown to be bona fide regulators of cardiac hypertrophy associated with mechanical stress and neuroendocrine stimulation [13]. The Trpc channels are Ca^{2+}-permeable, nonselective cation channels, which are controlled by a G protein-coupled receptor and mediate part of the store-operated Ca^{2+} entry in myocytes [17, 18]. Functional Trpc channels are homo- or heterotetramers [19, 20]. Several Trpc channels have been recognized as candidate sources of elevated $[Ca^{2+}]_i$ in cardiac hypertrophy [13, 21]. Hence, Trpc3 and Trpc6 have been implicated as central players leading to Ca^{2+} influx and Cn/NFAT activation during progression of cardiac hypertrophy [22, 23]. The resulting cation flux depolarizes the plasma membrane, leading to activation of voltage-dependent L-type Ca^{2+} channels, which causes a huge influx of Ca^{2+} that activates the Cn/NFAT pathway and hypertrophic responses in neonatal cardiomyocytes [23].

The L-type Ca^{2+} channel, which plays a critical role in regulating Ca^{2+}-dependent excitation–contraction coupling, is the primary Ca^{2+} influx pore in cardiac myocytes, and is associated with hypertrophic signaling. Under pathologic conditions, stimulated neurohumoral systems increase L-type Ca^{2+} current. Enhanced current is required for myocyte hypertrophy induced by isoproterenol [24], endothelin-1 [25], and angiotensin II [23]. Beneficial effects of voltage-gated Ca^{2+}-channel antagonists on cardiac hypertrophy and heart failure support the role of the L-type Ca^{2+} channel as a source of Ca^{2+} required to activate pathologic signaling [26, 27]. A study overexpressing the cardiac-specific β2 subunit of $Ca_V1.2$ showed that increasing L-type $Ca_V1.2$ current is sufficient to induce myocyte hypertrophy through activation of the Cn/NFAT and CaMKII/HDAC signaling pathways [26].

Here, we demonstrated that *Trpc3*$^{-/-}$ mice showed slightly decreased systolic BP and particular resistance to induction of pathologic cardiac hypertrophy and heart failure brought about by continuously elevated phenylephrine (PE) concentration. This was traced, at least in part, to reduced expression of $Ca_V1.2$, revealing an unexpected regulation of $Ca_V1.2$ expression and function by Trpc3.

Materials and methods

Mice

Generation of 129svev *Trpc3-/-* mice was described previously [28]. All animals analyzed in this study were maintained and in accordance with approved guideline and maintained according to the Yonsei Medical Center animal research requirements, and all procedures were approved by the Committee on Animal Research at Yonsei Medical Center (protocol number 2013-0237, 10-037). Mice were fed ad libitum and housed under a 12-h light cycle. Mice between 8 and 12 weeks of age were used for experiments. All experimental procedures were reviewed and approved by the Institutional Animal Research Ethics Committee at the Yonsei Medical Center (Seoul, South Korea). Because *Trpc3*$^{-/-}$ mice were fertile, so each 129svev WT line and *Trpc3*$^{-/-}$ line of mice were maintained independently. WT and *Trpc3*$^{-/-}$ mice born at same week were used as littermate. Body weight of WT and *Trpc3*$^{-/-}$ mice used in this study were not different and the body weight of 4 group were not also different at the before the pump implantation. (WT-PBS, 25.8 ± 2.5; WT-PE, 25.33 ± .3.0; *Trpc3*$^{-/-}$-PBS, 25.06 ± 1.3; *Trpc3*$^{-/-}$-PE, 25.70 ± 2.2).

Osmotic pump implantation and BP measurement

An Alzet 2200 pump implanted in the abdominal cavity of a wild-type (WT) and *Trpc3*$^{-/-}$ male 129sv mouse was used to infuse 65 mg PE/kg/day or 1.44 mg Angiotensin/kg/day for 28 days. Phosphate-buffered saline (PBS) was used for vehicle and control. Mouse BP was measured with noninvasive equipment, the two-chamber model of the BP-2000 BP analysis system (Visitech, Apex, NC, USA). Mice were adapted to caging in the measuring chamber and trained for tail cuff manipulation for 2 weeks before initiation of experiments. We monitored BP for approximately 3 weeks

before osmotic pump implantation. After implantation, mice were allowed to recover for 5 days, and then BP was monitored for 4 weeks. The stage platforms were heated to 37 °C. Ten primary BP measurements were taken, and 25 actual measurements were recorded. A minimum of five successful daily measurements were used in subsequent analyses.

Arterial constriction analysis of mesenteric artery

The lumen diameter measurement methods were described in the previous study [29]. Briefly, 150–200 nM in inner diameter, 2–3 mm in length of intact mesenteric artery were cannulated in a pressure-controlled myograph (Living Systems Instrumentation, Burlington, VT, USA), and the vessel responses to each concentration of PE were monitored by an inverted microscope (Eclipse TS100/TS100-F, Nikon Inc., Melville, NY, USA). The KH perfusion (luminal side of vessel) and superfusion (outside of vessel) of the arterial segments were equilibrated with a 95 % O_2 and 5 % CO_2 gas mixture at 37 °C. The mesenteric arterial segments were equilibrated for 40–60 min, after having been stretched out to their approximate natural length, then the arterial lumen diameter was recorded using the Soft Edge Acquisition Subsystem (IonOptix, Milton, MA, USA). The integrity of each vessel was preconfirmed at the beginning of each experiment with 70 mM K + solution containing Ca^{2+}, which was used to observe the maximal contraction activity of vessels (set at 100 %). Then, the integrity of vessels was postconfirmed at the end of the experiment, induced by 70 mM K^+ solution without Ca^{2+} in order to observe the full relaxation state of vessels. 3–5 independent experiments of each condition were summarized and the statistical significances were evaluated.

Hematoxylin and eosin (H&E) staining

Mice were anesthetized with a mixture of ketamine (100 mg/kg)/rumpun (2.5 mg/kg) via IP injection, and perfused with PBS alone or fixative (4 % v/v formaldehyde in PBS) to remove blood or fix tissue, respectively. Hearts were fixed for 24 h, embedded in paraffin, and sliced into 5-μm sections. H&E staining were performed to compare morphology of hearts and hypertrophy of cardio myocytes. Average cardio myocyte size was calculated by the ratio of the eosin-stained area to number of nuclei. 6–8 images of left ventricles were captured and analyzed using Metamorph software.

Echocardiographic analysis

Prior to transthoracic echocardiography, the left anterior chest wall was shaved and ultrasound gel applied. Mice were anesthetized with isoflurane, and echocardiography was performed using transthoracic 2-dimensional guided M-mode echocardiography by single, experienced echocardiographer. M-mode images were taken at the location of papillary muscles. Measurements were taken in triplicate, before and after implantation of the osmotic pump, from at least four mice for analysis.

Isolation and culture of primary neonatal cardiomyocytes

Neonatal cardiomyocytes form WT and *Trpc3*$^{-/-}$ male were isolated from 1-day-old mice heart. Their genotype was later identified using genomic DNA from their tail after primary culture of cardiomyocyte. Hearts were collected, minced, and incubated with 0.03 % (w/v) collagenase (Gibco-BRL 17101-015; Invitrogen) and 0.06 % (w/v) pancreatin (P-3292; Sigma-Aldrich, St. Louis, MO, USA) in Ads buffer (mmol/L: 116.4 NaCl, 20 HEPES, 1 NaH_2PO_4, 5.6 Glucose, 5.4 KCl, and 0.4 $MgSO_4$, adjusted to pH 7.35 with 5 N NaOH and 310 mOsm with 5 N NaCl) for 20 min at 37 °C. Purified cells were incubated in culture medium containing 10 % (v/v) FBS for 24 h, and then treated with 48 h. For *Trpc3*-siRNA-mediated knockdown, cells were incubated for 48–72 h after siRNA transfection.

Immunoblotting

Antibodies directed against $Ca_V1.2$ (ACC-033; Alomone, Jerusalem, Israel), β-actin (SC-1616), Trpc1 (SC-11376; Santa Cruz Biotechnology, Santa Cruz, CA, USA), and Trpc6 (SAB2102583; Sigma) were used for western analyses. Total heart or cardiomyocytes were extracted in lysis buffer (mmol/L: 150 NaCl, 5 NaEDTA, 10 % glycerol, 20 Tris–HCl [pH 8.0], 0.5 % Triton X-100, and proteinase inhibitors (Complete, Roche Applied Science, Indianapolis, IN, USA)). Protein lysates were separated on 4–12 % premade gradient SDS-PAGE gels (Komabiotech, Seoul, Korea) and transferred to membranes. Membranes were incubated in blocking solution (T-TBS containing 5 % nonfat milk) for 30 min at RT. After incubation with appropriate primary and secondary antibodies, protein bands were detected using enhanced chemi-luminescence reagents (Amersham Bioscience; GE Healthcare). Quantification of protein expression was based on measurement of band intensity using MultiGauge software (Fuji Film, Tokyo, Japan). Immunostaining results were quantified based on intensity of fluorescence in confocal microscopic images using Metamorph software (Molecular Devices, Sunnyvale, CA, USA).

RT-PCR and qPCR analyses

Total RNA was isolated from whole mouse hearts by homogenization in Trizol reagent and isopropanol was

used for RNA precipitation with isopropanol. Mouse-specific TaqMan® probes (for $Ca_V1.2$, Mm01188822; β-MHC, Mm01255770; ANP, Mm01255747; BNP, Mm01255770; 18S rRNA, Hs03928985; all from Life Technologies) were used in reverse transcription, real-time PCR. CDNA was synthesized in 20 μL from 1 μg total RNA using a cDNA synthesis kit, AffinityScript QPCR cDNA Synthesis Kit (Stratagene, La Jolla, CA, USA), and 0.1 μL cDNA was used for each qPCR reaction.

Statistical analysis

Results from multiple experiments are presented as mean ± SEM. Statistical analysis was performed using Student's *t* test or analysis of variance followed by Tukey's multiple comparison tests. $p < 0.05$ was considered statistically significant.

Results

Low BP and decreased PE-induced vessel contraction in *Trpc3*$^{-/-}$ mesenteric artery

To analyze the effect of *Trpc3* deletion on the cardiovascular system, we inserted a PBS- or PE-infusing osmotic pump (65 mg/kg/day) in the abdominal cavities of 129sv WT and *Trpc3*$^{-/-}$ mice, infused the mice for 4 weeks to mimic abnormal neurohumoral stimulation, and traced the BP change (Fig. 1a). *Trpc3*$^{-/-}$ mice showed slightly, but statistically significantly, lower systolic BP than WT in normal condition (Fig. 1b, before). Increased systolic BPs about 6–12 days after PE infusion was also lower in *Trpc3*$^{-/-}$ than in WT mice (Fig. 1b, maximum). Most importantly, BPs of PE-infused WT mice decreased dramatically after reaching maximum BP and were significantly lower than those of any other group (Fig. 1b, at end). Moreover, some PE-infused WT mice died before the end of infusion. These phenomena are mimic symptoms of heart failure after abnormal neurohumoral stimulation. In contrast, PE-infused *Trpc3*$^{-/-}$ mice also showed increased BP after PE infusion, but maximum systolic BPs were significantly lower than those of WT and returned to normal at the end of infusion, similar to the PBS-infused groups. In addition, PE-infused WT mice showed significantly reduced diastolic blood pressure and PE-infused *Trpc3*$^{-/-}$ mice did not show much difference with PBS-infused mice (supplementary Fig. 1). These findings indicate that Trpc3 contributes to BP regulation and mediates heart failure under conditions of abnormal neurohumoral stimulation. Because BP is mainly determined by vascular resistance, we compared PE-induced vasoconstriction in the third branch of mesenteric arteries from PBS- or PE-infused WT and *Trpc3*$^{-/-}$ mice. Figure 2a shows examples of PE-induced, concentration-dependent vasoconstriction. The magnitude of vasoconstriction induced by 5 and 10 μmol/L PE in PBS-infused *Trpc3*$^{-/-}$ mice was significantly reduced (Fig. 2b). Neither vasoconstriction nor the wall/lumen ratio were different between PE-infused WT and *Trpc3*$^{-/-}$ vessels (Fig. 2c, d). These results show that PE-induced vasoconstriction of a resistance artery is relatively weak in *Trpc3*$^{-/-}$ mice, and that the reduced vessel contraction response might be the cause of the relatively low BP in these mice.

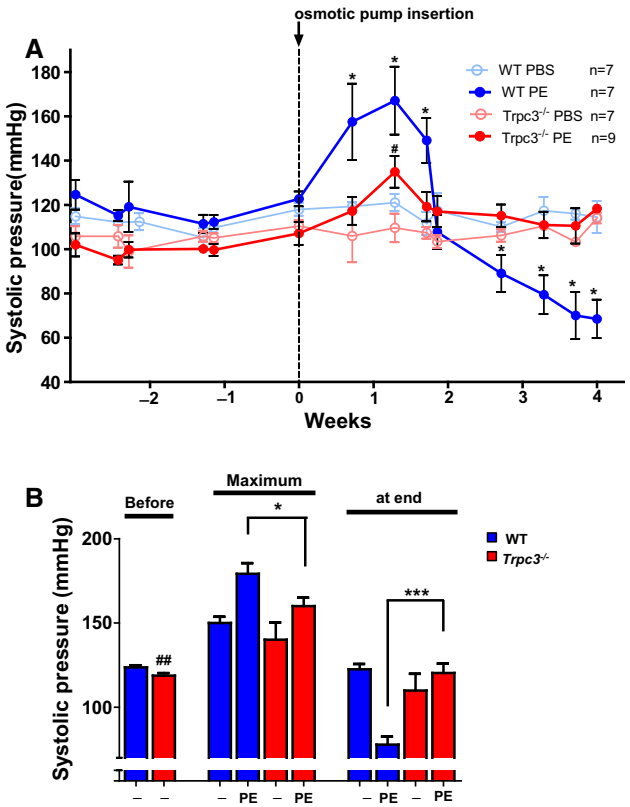

Fig. 1 The absence of phenylephrine-induced blood pressure-drop in *Trpc3*$^{-/-}$ mice. **a** Systolic blood pressures (BP) of WT and *Trpc3*$^{-/-}$ mice in PBS or PE infusion condition. Osmotic pump Alzet 2200 were inserted at 0 day (*arrow*) and PE were infused as 65 mg/kg/day. ($n = 7$–9). $^{*}p < 0.05$ compared with PBS-infused WT; $^{\#}p < 0.05$ compared with PBS-infused *Trpc3*$^{-/-}$ mice. **b** The summary of BP at the before osmotic pump implantation (Before), maximally elevated (Maximum), and last measurement (at end). Values represent mean ± SEM. $^{*}p < 0.05$, $^{***}p < 0.001$, and $^{\#\#}p < 0.001$ compared with PBS-infused WT

Absence of pathologic cardiac hypertrophy in *Trpc3*$^{-/-}$ mice

Suspecting that the sudden decrease of blood pressure might be caused by heart failure derived from deformation of the heart with elevated PE, we monitored several

indicators of pathologic cardiac hypertrophy. Pathologic cardiac hypertrophy was assessed based on heart per body weight ratio and morphological changes after H&E staining (Fig. 3a). The PE-infused WT hearts showed significant increase of heart/body weight ratio and dramatic morphological changes. The left ventricles were much thicker, and right ventricles were dilated. In contrast, *Trpc3*$^{-/-}$ mouse hearts showed the lower level of hypertrophy in PE-infused condition, but no significant pathologic differences were observed in heart/body weight ratio and morphology. To analyze hypertrophy in more detail, enlargement of cardiomyocyte and fibrosis in tissues were analyzed. Hearts were sectioned, stained with H&E, and observed at high magnification. Average cardiomyocyte size was calculated by the ratio of the eosin-stained area to number of nuclei (supplementary Fig. 2a, b). Cardiomyocyte in PE-infused WT ventricles exhibited greater than 2-fold enlargement compared to PBS-infused WT ventricles. Cardiomyocyte size in *Trpc3*$^{-/-}$ hearts was also slightly increased by PE, but the change was much smaller than observed in WT mice (supplementary Fig. 2b). To confirm the anti-hypertrophic result of *Trpc3*$^{-/-}$ mouse, AngII was infused for 28 days and the hearts were observed. AngII-infused WT hearts also showed hypertrophic heart/body weight ratio although they did not show the morphological changes as PE-infused mice showed (Fig. 3c, d). Whereas, *Trpc3*$^{-/-}$ mouse hearts did not show hypertrophic increase. These data demonstrate that Trpc3 is required for development of heart hypertrophy under conditions of abnormally elevated neurohumoral conditions.

Cardiac dysfunction and expression of markers of pathologic hypertrophy were absent in *Trpc3*$^{-/-}$ mice

Cardiac dysfunction is the most critical indicator of a pathologic state of the heart, and was assessed, here, based on percentage of fraction shortening (%FS) (Fig. 4a–c). M-mode echocardiogram images were taken at the level of the papillary muscles using echocardiography for small

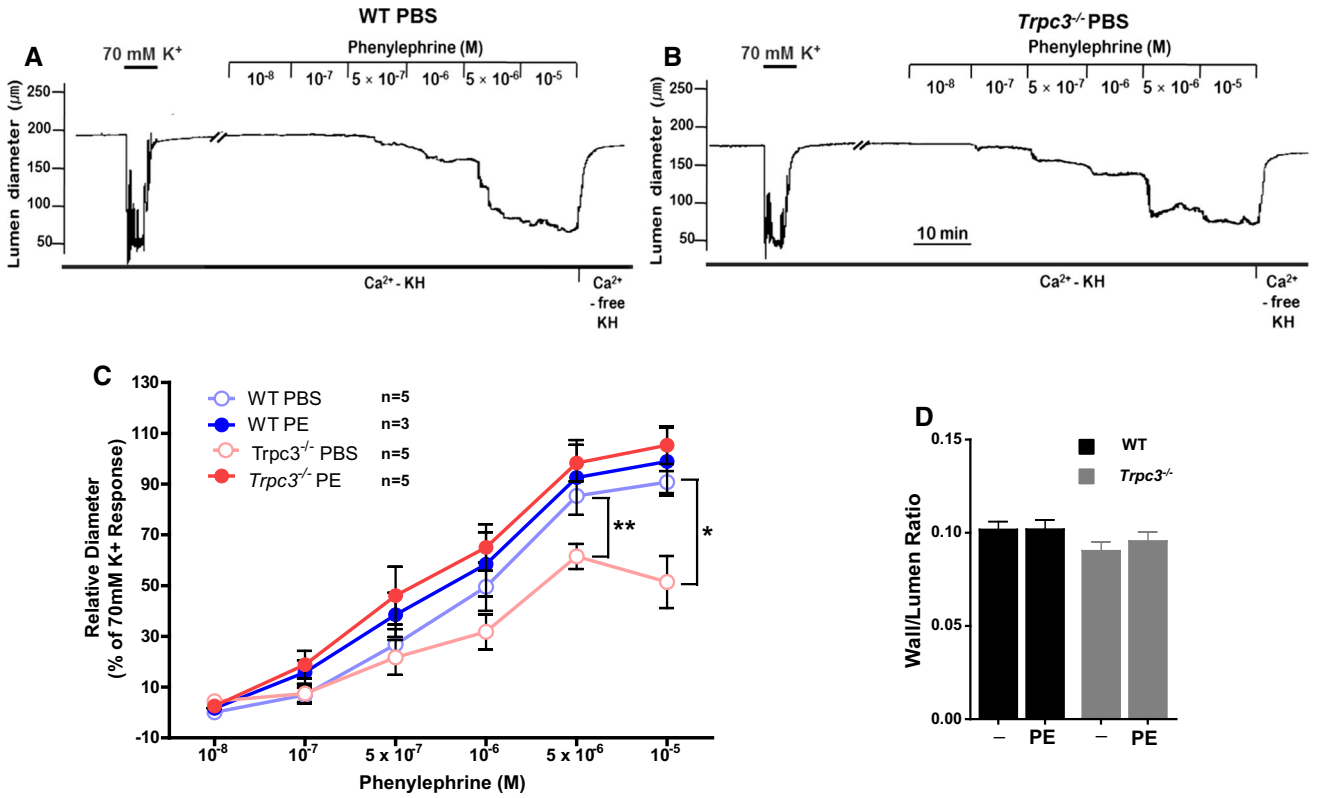

Fig. 2 PE-stimulated vasoconstriction was decreased in *Trpc3*$^{-/-}$ mesenteric artery. **a–b** Representative recording traces of PE-induced vasoconstriction of arteries from WT(A) and *Trpc3*$^{-/-}$ mice (**b**) infused with PBS. The lumen diameter (Y *axis*) of vessel cannulated in the intraluminal pressure-controlled arteriography devises was shown in various concentrations of PE. The vessel relaxation caused by C^{2+}-free KH treatment proved the integrity of the vessel contraction response at the end of the experiment.**c** Summary of mean data for PE-induced vasoconstriction in WT and *Trpc3*$^{-/-}$ mice infused with PBS or PE. Relative contraction activity was normalized to the maximal vasoconstriction induced by 70 mmol/L K^+ with Ca^{2+} (not shown in **a** and **b**) which defined as 100 % activity. Data represent mean ± SEM of three to five independent experiments. **d** Arterial-wall thickness/lumen diameter in WT and *Trpc3*$^{-/-}$ mice infused with PBS (−) or PE. Values represent mean ± SEM (n = 5–10). Vessel diameter was measured at an intraluminal pressure of 40 mmHg."

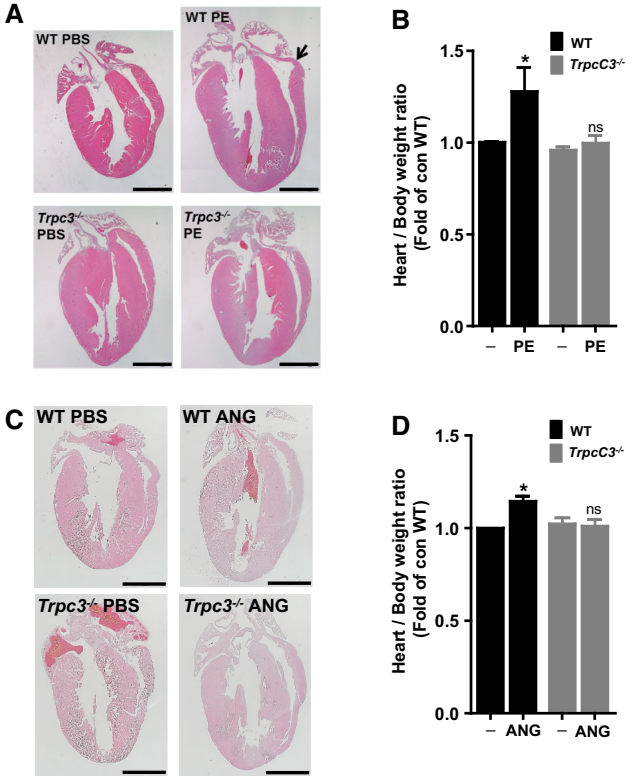

Fig. 3 Reduced heart hypertrophy by elevated PE or AngII in *Trpc3*$^{-/-}$ mice. a Heart morphology of WT and *Trpc3*$^{-/-}$ mice after phenylephrine (PE) infusion using H&E staining. *Arrow* in **a** indicates dilated right ventricle. **b** Heart/body weight ratio of wild-type (WT) and *Trpc3*$^{-/-}$ mice after phenylephrine (PE) infusion. **c** Heart morphology of WT and *Trpc3*$^{-/-}$ mice after angiotensin II (AngII) infusion. **d** Heart/body weight ratio of wild-type (WT) and *Trpc3*$^{-/-}$ mice after AngII infusion. Values represent mean ± SEM. *$p < 0.05$ in (**b**) and (**d**) compared with PBS-infused WT mice; ns compared with PBS-infused *Trpc3*$^{-/-}$ mice

animals and used for %FS calculation. Before osmotic pump implantation, %FS was similar in WT and *Trpc3*$^{-/-}$ mice (Fig. 4b). Interestingly, %FS of WT mice was significantly decreased after 3 weeks of PE infusion, but that of *Trpc3*$^{-/-}$ mice was either unchanged or slightly increased (Fig. 4c). These findings suggest that the PE-induced functional heart abnormality developed only in WT mice. An important feature of decreased heart function with hypertrophy is induction of the molecular stress fetal gene program. Representative markers of that program under conditions of cardiac stress are induction of certain mRNAs, such as β-MHC, ANF, and BNP [14, 30]. We measured levels of these mRNAs in hearts of WT and *Trpc3*$^{-/-}$ mice infused with PBS or PE by quantitative RT-PCR (Fig. 4d–f). Only PE-infused WT hearts showed marked increases in expression of β-MHC, ANP, and BNP mRNA. Interestingly, PBS-infused *Trpc3*$^{-/-}$ mice showed more expression of three markers than WT and no increase (β-MHC and ANP), or a small decrease (BNP) in PE-infused condition. These results indicate that pathologic cardiac hypertrophy developed in PE-infused WT hearts, but PE-infused *Trpc3*$^{-/-}$ hearts were protected from activation of pathologic genes expression. Together, these analyses of morphology, function, and hypertrophic marker expression clearly demonstrate that *Trpc3* deletion prevents development of pathologic cardiac hypertrophy caused by elevated neurohumoral stimulation.

Low basal and PE-induced expression of $Ca_V1.2$ in *Trpc3*$^{-/-}$ hearts

Western analysis unexpectedly showed that expression of L-type Ca^{2+} channel protein $Ca_V1.2$ was significantly lower in *Trpc3*$^{-/-}$ than in WT hearts, and PE-induced expression of $Ca_V1.2$ was nearly absent (Fig. 5a, b). In addition, $Ca_V1.2$ mRNA expression in *Trpc3*$^{-/-}$ heart was greatly reduced compared with WT heart (Fig. 5c; $^{\#\#}p < 0.01$). Interestingly, PE induced a nearly 3-fold increase in $Ca_V1.2$ mRNA expression in WT heart. An increase was seen in *Trpc3*$^{-/-}$ hearts ($^{\&}p < 0.05$), although the absolute amount of induced mRNA was much less than in WT (Fig. 5c; $^{**}p < 0.01$). In contrast, Trpc1 and Trpc6 protein expression were not different in WT and *Trpc3*$^{-/-}$ hearts and elevated PE had no noticeable effect on these expression patterns (Fig. 5d–f). Because of the no obvious functional abnormality in normal *Trpc3*$^{-/-}$ hearts (Fig. 4b) despite of the decreased $Ca_V1.2$ expression, we searched for altered expression of contraction-related proteins that might compensate for decreased $Ca_V1.2$ expression, but found no changes in excitation–contraction–related proteins, at least at the mRNA level (supplementary Fig. 3). These results suggested that decreased basal expression and attenuated PE-induced expression of $Ca_V1.2$ in *Trpc3*$^{-/-}$ hearts might contribute the resistance to pathological cardiac hypertrophy and heart failure in *Trpc3*$^{-/-}$ mice.

$Ca_V1.2$ expression is dependent on the presence and activity of TRPC3

Finally, to determine whether $Ca_V1.2$ expression is dependent on Trpc3, we tested the effect of siRNA-mediated *Trpc3* knockdown and OAG stimulation of Trpc3 on $Ca_V1.2$ protein expression in isolated cardiomyocytes (Fig. 6a, c). The reduction of *Trpc3* mRNA by siRNA for *Trpc3* was confirmed by RT-PCR analysis (Fig. 6b). OAG treatment resulted in increased $Ca_V1.2$ expression, and *Trpc3* knockdown significantly reduced $Ca_V1.2$ expression. Moreover, *Trpc3* knockdown eliminated the OAG-induced increase in $Ca_V1.2$ expression. These results indicate that

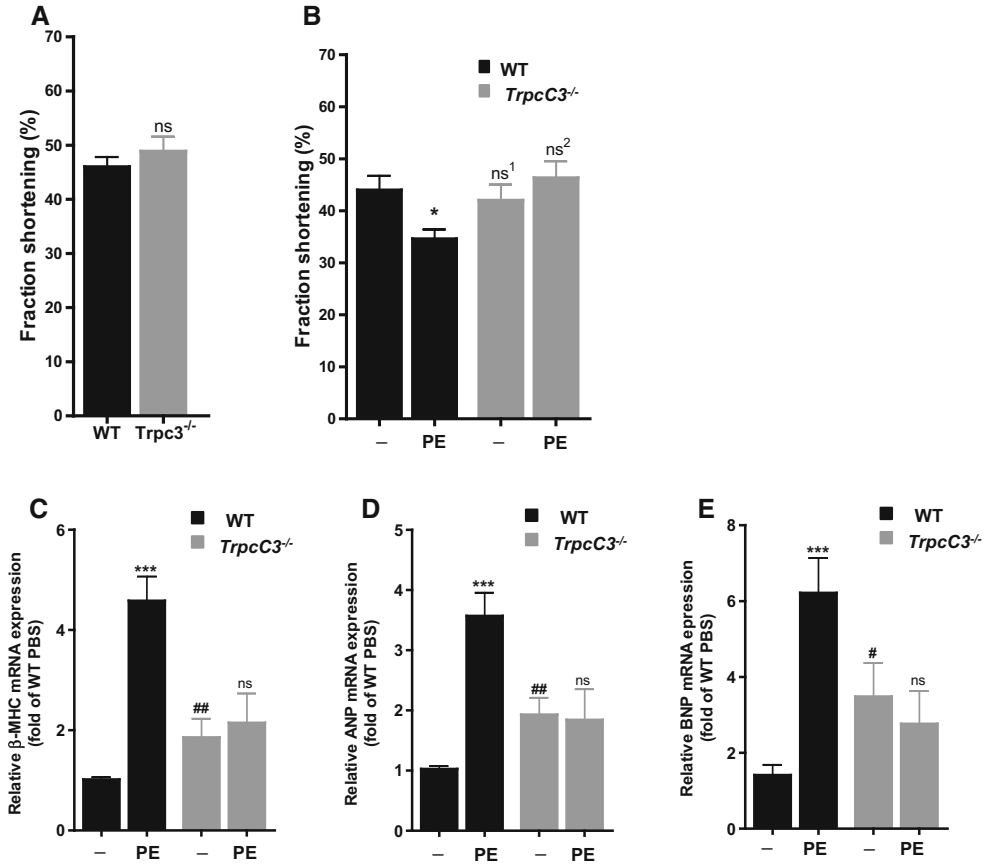

Fig. 4 The absence of pathologic hypertrophic symptoms in *Trpc3*$^{-/-}$ mice. **a** Representative image of the echocardiography **b**–**c** Fraction shortening (%) measured by echocardiography in WT and *Trpc3*$^{-/-}$ mice. %FS of before (**b**) and after (**c**) PE infusion were summarized. Values represent mean ± SEM; ns in (**b**) compared with PBS-infused WT mice; *$p < 0.05$ and ns^1 in (**c**) compared with WT-PBS-infused mice; ns^2 compared with PBS-infused *Trpc3*$^{-/-}$ mice. **d**–**f** Gene expression of cardiac hypertrophy markers: β-myosin heavy chain (β-MHC) (**d**), atrial natriuretic factor (ANF) (**e**), and brain natriuretic peptide (BNP) (**f**) normalized to 18S ribosomal RNA, in WT and *Trpc3*$^{-/-}$ mice after PBS or PE infusion. ***$p < 0.001$ in (**d**, **e**, and **f**) compared with PBS-infused WT mice; $^{\#\#}p < 0.001$ in (**d** and **e**) and $^{\#}p < 0.05$ in (**f**) compared with PBS-infused WT; ns in (**d**, **e**, and **f**) compared with PBS-infused *Trpc3*$^{-/-}$ mice

$Ca_V1.2$ expression is dependent on Trpc3 expression and activity.

Discussion

Among Trpc channels, Trpc3 and Trpc6 have been extensively analyzed in relation to their pathologic effects on the cardiovascular system [3, 5, 15, 16, 23]. Stimulation by neuroendocrine agonists or by pressure overload causes cardiac hypertrophy in mice with cardiac-specific overexpression of Trpc3 [15] or Trpc6 [5]. In addition, mice expressing cardiac-specific dominant-negative Trpc3 or Trpc6 mutants showed attenuated cardiac hypertrophy [3]. However, paradoxically, whole deletion of Trpc6 (*Trpc6*$^{-/-}$) mice showed elevated BP and enhanced agonist-induced vessel contractility. Therefore, we elucidated the role of systemic *Trpc3* deletion in blood pressure and cardiac remodeling especially in elevated neurohumoral condition. Here, we found *Trpc3*$^{-/-}$ mice display resistance to cardiac hypertrophy under stimulated neurohumoral conditions, such as elevated PE or AngII. Our morphology (Fig. 3a, b), function (Fig. 4a–c), and pathologic marker expression analysis (Fig. 4d–f) revealed that Trpc3 is required for development of pathological heart hypertrophy under conditions of abnormally elevated PE. Daily systolic pressure measurement during 2 weeks of normal resting conditions and 4 weeks of PBS infusion revealed that *Trpc3*$^{-/-}$ mice are slightly hypotensive. In addition, PE-induced increase in BP of *Trpc3*$^{-/-}$ mice was much smaller than that of WT (Fig. 1). The sudden decrease of blood pressure was only observed in PE-infused WT mice, which might be caused by heart failure derived from deformation of the heart in elevated PE condition and our data proved that PE-infused WT mice heart were experienced pathologic hypertrophy, but PE-

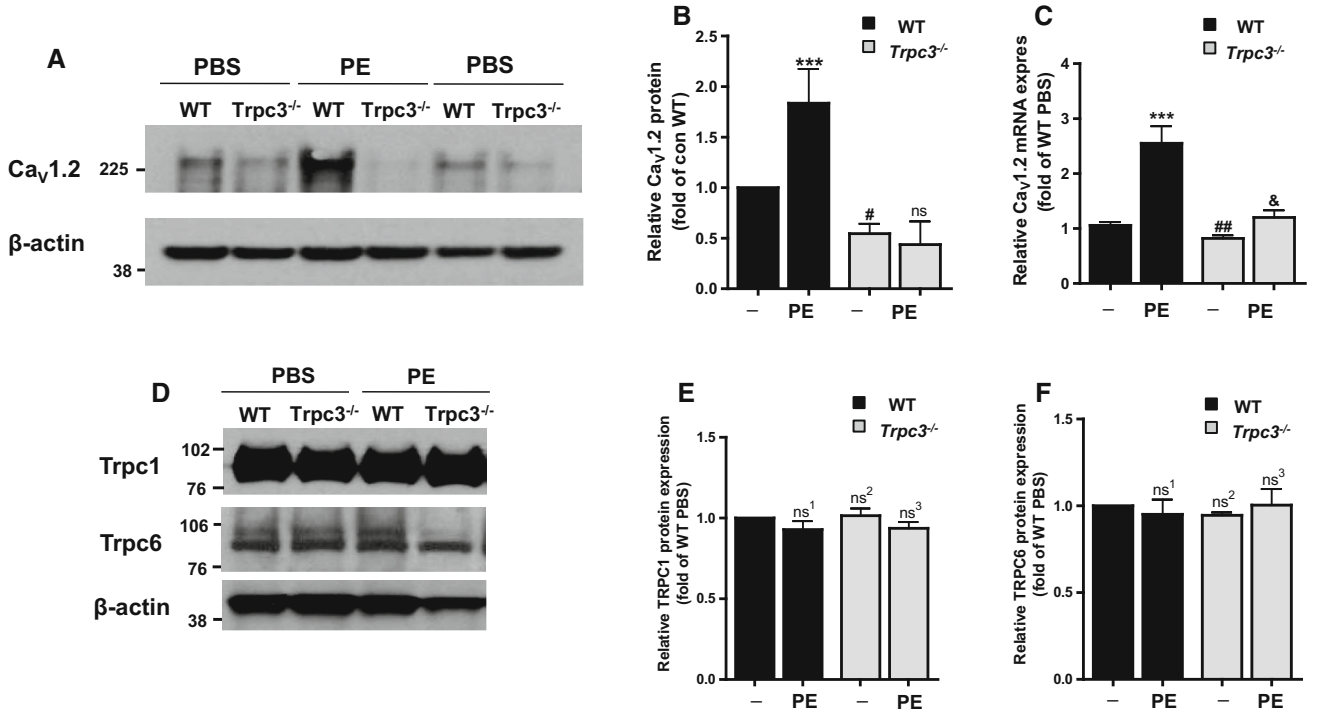

Fig. 5 Basal- and PE-induced expression of $Ca_V1.2$ were decreased in *Trpc3*$^{-/-}$ Heart. **a**–**b** Reduced $Ca_V1.2$ expression in PBS-infused heart and lack of up-regulation by PE infusion in hearts of *Trpc3*$^{-/-}$ mice. Western analysis **a** and quantitation **b** of $Ca_V1.2$ in heart lysates from WT and *Trpc3*$^{-/-}$ mice treated with PBS or PE. Blots are representative and values represent mean ± SEM of three independent experiments. $^{***}p < 0.0001$ and $^{\#}p < 0.05$ compared with PBS-infused WT mice; ns compared with PBS-infused *Trpc3*$^{-/-}$ mice. **c** RT-PCR analysis of relative $Ca_V1.2$ mRNA levels of WT and *Trpc3*$^{-/-}$ mice heart treated with PBS or PE. No significant inducible expression of mRNA was detected in *Trpc3*$^{-/-}$ mice. $^{***}p < 0.001$ and $^{\#\#}p < 0.01$ compared with PBS-treated WT mice; $^{\&}p < 0.05$ compared with PBS-infused *Trpc3*$^{-/-}$ mice. **d**–**f** Western analysis (**d**) and quantitation of Trpc1 (**e**) and Trpc6 (**f**) in each groups. ns^1, ns^2 compare with PBS-infused WT mice; compared with ns^3 compared with PBS-infused *Trpc3*$^{-/-}$ mice

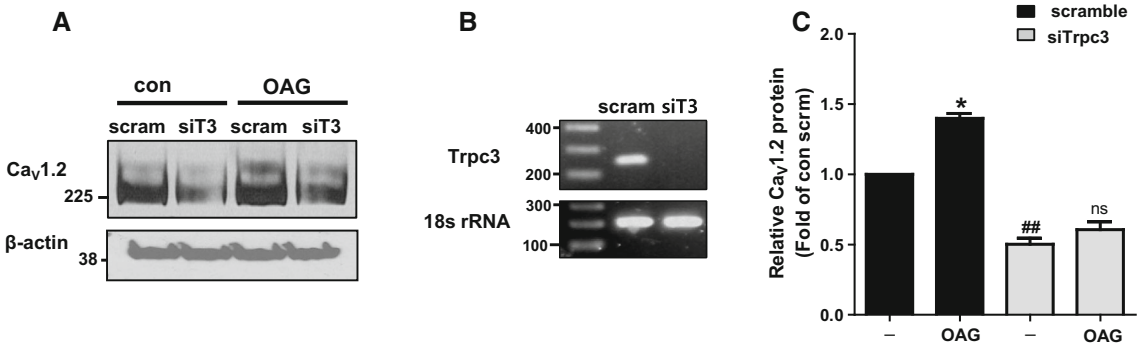

Fig. 6 Cardiac $Ca_V1.2$ expression and activity depends on the presence and activity of Trpc3. **a** Trpc3 and its activator, OAG regulates $Ca_V1.2$ expression in primary cultured neonatal cardiomyocytes. Western analysis of $Ca_V1.2$ expression in primary cultured neonatal cardiomyocytes transfected with scrambled (scram) control siRNA or siRNA targeting *Trpc3* (siT3) and incubated in the presence or absence of 100 μmol/L OAG for 24 h. β-actin served as internal control. **b** RT-PCR analysis of *Trpc3* mRNA in primary cultured neonatal cardiomyoctyes transfected with scrambled control siRNA or siRNA targeting *Trpc3*; 18 s RNA served as internal control. **c** Quantitation of results of western analysis of $Ca_V1.2$ expression in WT and *Trpc3*$^{-/-}$ primary cultured neonatal cardiomyocytes transfected with control siRNA or siRNA targeting *Trpc3* and incubated in the presence or absence of OAG. Values represent mean ± SEM of three independent experiments; $^{*}p < 0.05$ and $^{\#\#}p < 0.01$ compared with con scramble treated condition; ns compared with con siTrpc3-treated condition

infused *Trpc3*$^{-/-}$ mice were not (Fig. 1 and Fig. 3a, b). These data clearly demonstrated that TRPC3 mediates pathologic hypertrophy in heart in elevated PE condition.

Physiologically, reduced sensitivity of resistance vessels to a constrictor (PE) results in lower elevated mean arterial BP [31]. Therefore, the lower BP seen in PE-infused

Trpc3$^{-/-}$ mice was probably caused by the reduced vasocontractility of *Trpc3*$^{-/-}$ mice, as shown in Fig. 2. The positive effect of Trpc3 on vessel contraction was also reported in our previous study, which showed that Trpc3 mediates PE-induced vasoconstriction that may contribute to the elevated BP in pseudo-hypoaldosteronism type 2 (PHAII) hypertension, a rare autosomal dominant disorder featuring hypertension associated with hyperkalemia, based on the studies of PHAII-causing mutants of WNK4 kinase [32]. Conversely, 2 out of 7 PE-infused WT mice died near the end of infusion due to heart failure, and their right ventricles were severely dilated, which is the representative phenotype of pulmonary hypertension [33]. In addition, *Trpc3* mRNA and protein expression in pulmonary artery smooth muscle cells from idiopathic pulmonary artery hypertension patients were much higher than in those from normotensive patients [34]. Hence, it is possible that the absence of Trpc3 in the pulmonary artery might have contributed to the observed low BP. The effect of *Trpc3* deletion on pulmonary artery is currently under investigation in our laboratory.

Trpc3$^{-/-}$ hearts displayed low $Ca_V1.2$ protein expression, which was not inducible by PE (Fig. 5a, b). Trpc3-dependent expression of $Ca_V1.2$ was demonstrated by marked reduction of $Ca_V1.2$ expression and the absence of OAG induction of $Ca_V1.2$ expression using siRNA-mediated *Trpc3* knockdown in cardiomyocytes (Fig. 6a, c). It appears that Trpc3 regulates $Ca_V1.2$ primarily through transcriptional control via the Ca^{2+}/Cn/NFAT system because $Ca_V1.2$ mRNA expression was low in *Trpc3*$^{-/-}$ heart, and PE-induced $Ca_V1.2$ mRNA expression was also attenuated (Fig. 5c). Hui Gao et al. recently reported the blockade of Trpc3-induced Cn/NFAT activation and myocyte hypertrophy by a selective L-type Ca^{2+} channel blocker [35] showed an accordance with our findings. In addition to their report, our results extended that direct alterations in Cav1.2 expression in response to TRPC3 knockdown and stimulation.

It is unexpected observation that deletion of one type of Ca^{2+} influx channel, Trpc3, abrogates the expression of another, $Ca_V1.2$, as found in *Trpc3*$^{-/-}$ heart. Nevertheless, this phenomenon is possible because the two channel types could form a signaling complex in a specialized cell surface micro-domain. $Ca_V1.2$ physically interacts with Trpcs, and this interaction affects the pace-making and electrical activity of chick embryonic hearts [7]. In addition, Trpc1 and Trpc3–7 may form multiple complexes with the endogenous $Ca_V1.2$ channel α1C subunit in the atrium and ventricle [7]. Moreover, Trpc3 and $Ca_V1.2$ are found in a specialized micro-domain of lipid rafts that serve as signal transduction organizing centers [36, 37]. Therefore, it will be interesting to identify the protein level interaction of TRPC3 and $Ca_V1.2$. It is possible that their coexistence in a complex contributes not only to protein stability, but also to more efficient signal transduction yielding more efficient Ca^{2+} entry. Efficient Ca^{2+} entry might promote higher Ca^{2+}/NFAT3 activation and increased transcription of $Ca_V1.2$. Moreover, the high affinity NFAT binding sites were found only in the cardiac promoter of $Ca_V1.2$, which is produced by alternative splicing [38, 39], so this feed-forward mechanism could only be found in the cardiaomyocyte. Therefore, this feed-forward loop might exist only in micro-domains of cardiomyocytes where Trpc3 and $Ca_V1.2$ exist in a complex. Most importantly, this feed-forward circuit could synergistically act on the development of pathologic cardiac hypertrophy under conditions of abnormal neurohumoral stimulation as observed in WT hearts, but not in *Trpc3*$^{-/-}$ hearts.

Seo et al. reported that inhibition of both Trpc3 and Trpc6 are necessary to block TAC-induced hypertrophy, but *Trpc3* single deletion failed [40]. The discrepancy between their data and ours were caused by difference of background strain and stress condition (129sv strain in elevated PE condition for our study and the changed background strain from 129sv to C57BL6 by 5 generation backcross in TAC condition for their study). Different baseline cardiovascular phenotypes of these strains were well known [41] and especially, the different cardiac responses to pressure overload (TAC)-induced left ventricle hypertrophy between 129sv and C57BL6 strain were reported in detail [42]. Secondly, PE-infused *Trpc3*$^{-/-}$ hearts of our study showed slightly decreased expression of BNP expression than PBS infusion (Fig. 2e), whereas TAC subjected *Trpc3*$^{-/-}$ mice of their study showed elevated Nppa (ANP) and Nppb (BNP) expression. These results suggested that the different stresses of elevated PE and TAC conditions cause different effects on heart at least in *Trpc3*$^{-/-}$ mice. Therefore, it seems that TRPC3 mediates the additional pathologic effect by elevated PE which probably mediated by direct α1-adrenergic receptor activation in cardiomyocytes.

Increased *TRPC3* channels are observed in vascular endothelium of patients with essential hypertension [43], and the various Trpc-inhibitory compounds blocks cardiac hypertrophy in mice subjected to pressure overload [44]. These findings and ours suggest that TRPC3 inhibition is a promising candidate for treatment of hypertension and pathologic cardiac hypertrophy. Especially, present findings provide additional therapeutic significance of TRPC3 inhibition as a candidate for treating pathologic cardiac hypertrophy because of its effect on reducing cardiac $Ca_V1.2$ expression.

Acknowledgments We thank Jeungsik In in CPEC (Cardiovascular Product Evaluation Center) at Yonsei University Health System, Jangwoo Cho in SI healthcare and Heinmiller, Andrew in

VisualSonics Inc. for helping echocardiogram measurements and analysis. This work was supported by a National Research Foundation of Korea (NRF) Grant funded by the Korean government (No. NRF-2011-0029459 for JY KIM, MSIP-2013R1A3A2042197 for MG LEE) and the Intramural Research Program of the NIH (Project Z01-ES101864 to LB).

Compliance with ethical standards

Conflict of interest The authors state no conflict of interest.

References

1. McMurray JJ (2010) Clinical practice. Systolic heart failure. N Engl J Med 362:228–238. doi:10.1056/NEJMcp0909392
2. Jessup M, Brozena S (2003) Heart failure. N Engl J Med 348:2007–2018. doi:10.1056/NEJMra021498
3. Wu X, Eder P, Chang B, Molkentin JD (2010) TRPC channels are necessary mediators of pathologic cardiac hypertrophy. Proc Natl Acad Sci USA 107:7000–7005. doi:10.1073/pnas.1001825107
4. Wilkins BJ, Dai YS, Bueno OF, Parsons SA, Xu J, Plank DM, Jones F, Kimball TR, Molkentin JD (2004) Calcineurin/NFAT coupling participates in pathological, but not physiological, cardiac hypertrophy. Circ Res 94:110–118. doi:10.1161/01.res.0000109415.17511.18
5. Kuwahara K, Wang Y, McAnally J, Richardson JA, Bassel-Duby R, Hill JA, Olson EN (2006) TRPC6 fulfills a calcineurin signaling circuit during pathologic cardiac remodeling. J Clin Invest 116:3114–3126. doi:10.1172/jci27702
6. Horiba M, Muto T, Ueda N, Opthof T, Miwa K, Hojo M, Lee JK, Kamiya K, Kodama I, Yasui K (2008) T-type Ca2 + channel blockers prevent cardiac cell hypertrophy through an inhibition of calcineurin-NFAT3 activation as well as L-type Ca2 + channel blockers. Life Sci 82:554–560. doi:10.1016/j.lfs.2007.11.010
7. Sabourin J, Robin E, Raddatz E (2011) A key role of TRPC channels in the regulation of electromechanical activity of the developing heart. Cardiovasc Res 92:226–236. doi:10.1093/cvr/cvr167
8. Tandan S, Wang Y, Wang TT, Jiang N, Hall DD, Hell JW, Luo X, Rothermel BA, Hill JA (2009) Physical and functional interaction between calcineurin and the cardiac L-type Ca2 + channel. Circ Res 105:51–60. doi:10.1161/circresaha.109.199828
9. Semsarian C, Ahmad I, Giewat M, Georgakopoulos D, Schmitt JP, McConnell BK, Reiken S, Mende U, Marks AR, Kass DA, Seidman CE, Seidman JG (2002) The L-type calcium channel inhibitor diltiazem prevents cardiomyopathy in a mouse model. J Clin Invest 109:1013–1020. doi:10.1172/jci14677
10. Liao Y, Asakura M, Takashima S, Ogai A, Asano Y, Asanuma H, Minamino T, Tomoike H, Hori M, Kitakaze M (2005) Benidipine, a long-acting calcium channel blocker, inhibits cardiac remodeling in pressure-overloaded mice. Cardiovasc Res 65:879–888. doi:10.1016/j.cardiores.2004.11.006
11. Nuss HB, Houser SR (1994) Effect of duration of depolarisation on contraction of normal and hypertrophied feline ventricular myocytes. Cardiovasc Res 28:1482–1489
12. Cribbs LL, Martin BL, Schroder EA, Keller BB, Delisle BP, Satin J (2001) Identification of the t-type calcium channel (Ca(v)3.1d) in developing mouse heart. Circ Res 88:403–407
13. Eder P, Molkentin JD (2011) TRPC channels as effectors of cardiac hypertrophy. Circ Res 108:265–272. doi:10.1161/circresaha.110.225888
14. Seth M, Zhang ZS, Mao L, Graham V, Burch J, Stiber J, Tsiokas L, Winn M, Abramowitz J, Rockman HA, Birnbaumer L, Rosenberg P (2009) TRPC1 channels are critical for hypertrophic signaling in the heart. Circ Res 105:1023–1030. doi:10.1161/circresaha.109.206581
15. Nakayama H, Wilkin BJ, Bodi I, Molkentin JD (2006) Calcineurin-dependent cardiomyopathy is activated by TRPC in the adult mouse heart. FASEB J 20:1660–1670. doi:10.1096/fj.05-5560
16. Kinoshita H, Kuwahara K, Nishida M, Jian Z, Rong X, Kiyonaka S, Kuwabara Y, Kurose H, Inoue R, Mori Y, Li Y, Nakagawa Y, Usami S, Fujiwara M, Yamada Y, Minami T, Ueshima K, Nakao K (2010) Inhibition of TRPC6 channel activity contributes to the antihypertrophic effects of natriuretic peptides-guanylyl cyclase-A signaling in the heart. Circ Res 106:1849–1860. doi:10.1161/circresaha.109.208314
17. Clapham DE (2003) TRP channels as cellular sensors. Nature 426:517–524. doi:10.1038/nature02196
18. Yuan JP, Zeng W, Huang GN, Worley PF, Muallem S (2007) STIM1 heteromultimerizes TRPC channels to determine their function as store-operated channels. Nat Cell Biol 9:636–645,doi:10.1038/ncb1590
19. Strubing C, Krapivinsky G, Krapivinsky L, Clapham DE (2001) TRPC1 and TRPC5 form a novel cation channel in mammalian brain. Neuron 29:645–655
20. Hofmann T, Schaefer M, Schultz G, Gudermann T (2002) Subunit composition of mammalian transient receptor potential channels in living cells. Proc Natl Acad Sci U S A 99:7461–7466. doi:10.1073/pnas.102596199
21. Inoue R, Jensen LJ, Shi J, Morita H, Nishida M, Honda A, Ito Y (2006) Transient receptor potential channels in cardiovascular function and disease. Circ Res 99:119–131. doi:10.1161/01.RES.0000233356.10630.8a
22. Hofmann T, Obukhov AG, Schaefer M, Harteneck C, Gudermann T, Schultz G (1999) Direct activation of human TRPC6 and TRPC3 channels by diacylglycerol. Nature 397:259–263. doi:10.1038/16711
23. Onohara N, Nishida M, Inoue R, Kobayashi H, Sumimoto H, Sato Y, Mori Y, Nagao T, Kurose H (2006) TRPC3 and TRPC6 are essential for angiotensin II-induced cardiac hypertrophy. EMBO J 25:5305–5316. doi:10.1038/sj.emboj.7601417
24. Zou Y, Yamazaki T, Nakagawa K, Yamada H, Iriguchi N, Toko H, Takano H, Akazawa H, Nagai R, Komuro I (2002) Continuous blockade of L-type Ca2 + channels suppresses activation of calcineurin and development of cardiac hypertrophy in spontaneously hypertensive rats. Hypertens Res 25:117–124
25. Ikeda K, Tojo K, Tokudome G, Akashi T, Hosoya T, Harada M, Nakagawa O, Nakao K (2000) Possible involvement of endothelin-1 in cardioprotective effects of benidipine. Hypertens Res 23:491–496
26. Chen X, Nakayama H, Zhang X, Ai X, Harris DM, Tang M, Zhang H, Szeto C, Stockbower K, Berretta RM, Eckhart AD, Koch WJ, Molkentin JD, Houser SR (2011) Calcium influx through Cav1.2 is a proximal signal for pathological cardiomyocyte hypertrophy. J Mol Cell Cardiol 50:460–470. doi:10.1016/j.yjmcc.2010.11.012
27. Ago T, Yang Y, Zhai P, Sadoshima J (2010) Nifedipine inhibits cardiac hypertrophy and left ventricular dysfunction in response to pressure overload. J Cardiovasc Transl Res 3:304–313. doi:10.1007/s12265-010-9182-x
28. Hartmann J, Dragicevic E, Adelsberger H, Henning HA, Sumser M, Abramowitz J, Blum R, Dietrich A, Freichel M, Flockerzi V, Birnbaumer L, Konnerth A (2008) TRPC3 channels are required for synaptic transmission and motor coordination. Neuron 59:392–398. doi:10.1016/j.neuron.2008.06.009

29. Yeon SI, Kim JY, Yeon DS, Abramowitz J, Birnbaumer L, Muallem S, Lee YH (2014) Transient receptor potential canonical type 3 channels control the vascular contractility of mouse mesenteric arteries. PLoS ONE 9:e110413. doi:10.1371/journal.pone.0110413
30. Maillet M, van Berlo JH, Molkentin JD (2013) Molecular basis of physiological heart growth: fundamental concepts and new players. Nat Rev Mol Cell Biol 14:38–48. doi:10.1038/nrm3495
31. Dietrich A, Mederos YSM, Gollasch M, Gross V, Storch U, Dubrovska G, Obst M, Yildirim E, Salanova B, Kalwa H, Essin K, Pinkenburg O, Luft FC, Gudermann T, Birnbaumer L (2005) Increased vascular smooth muscle contractility in TRPC6-/- mice. Mol Cell Biol 25:6980–6989. doi:10.1128/mcb.25.16.6980-6989.2005
32. Park HW, Kim JY, Choi SK, Lee YH, Zeng W, Kim KH, Muallem S, Lee MG (2011) Serine-threonine kinase with-no-lysine 4 (WNK4) controls blood pressure via transient receptor potential canonical 3 (TRPC3) in the vasculature. Proc Natl Acad Sci U S A 108:10750–10755. doi:10.1073/pnas.1104271108
33. Rockman HA, Ono S, Ross RS, Jones LR, Karimi M, Bhargava V, Ross J Jr, Chien KR (1994) Molecular and physiological alterations in murine ventricular dysfunction. Proc Natl Acad Sci U S A 91:2694–2698
34. Yu Y, Fantozzi I, Remillard CV, Landsberg JW, Kunichika N, Platoshyn O, Tigno DD, Thistlethwaite PA, Rubin LJ, Yuan JX (2004) Enhanced expression of transient receptor potential channels in idiopathic pulmonary arterial hypertension. Proc Natl Acad Sci USA 101:13861–13866. doi:10.1073/pnas.0405908101
35. Gao H, Wang F, Wang W, Makarewich CA, Zhang H, Kubo H, Berretta RM, Barr LA, Molkentin JD, Houser SR (2012) Ca(2 +) influx through L-type Ca(2 +) channels and transient receptor potential channels activates pathological hypertrophy signaling. J Mol Cell Cardiol 53:657–667. doi:10.1016/j.yjmcc.2012.08.005
36. Ambudkar IS, Brazer SC, Liu X, Lockwich T, Singh B (2004) Plasma membrane localization of TRPC channels: role of caveolar lipid rafts. Novartis Found Symp 258:63–70; discussion (70–74, 98–102, 263–266)
37. Balijepalli RC, Foell JD, Hall DD, Hell JW, Kamp TJ (2006) Localization of cardiac L-type Ca(2 +) channels to a caveolar macromolecular signaling complex is required for beta(2)-adrenergic regulation. Proc Natl Acad Sci U S A 103:7500–7505. doi:10.1073/pnas.0503465103 discussion (70–74, 98–102, 263–266)
38. Saada N, Dai B, Echetebu C, Sarna SK, Palade P (2003) Smooth muscle uses another promoter to express primarily a form of human Cav1.2 L-type calcium channel different from the principal heart form. Biochem Biophys Res Commun 302:23–28
39. Saada NI, Carrillo ED, Dai B, Wang WZ, Dettbarn C, Sanchez J, Palade P (2005) Expression of multiple CaV1.2 transcripts in rat tissues mediated by different promoters. Cell Calcium 37:301–309. doi:10.1016/j.ceca.2004.11.003
40. Seo K, Rainer PP, Shalkey Hahn V, Lee DI, Jo SH, Andersen A, Liu T, Xu X, Willette RN, Lepore JJ, Marino JP Jr, Birnbaumer L, Schnackenberg CG, Kass DA (2014) Combined TRPC3 and TRPC6 blockade by selective small-molecule or genetic deletion inhibits pathological cardiac hypertrophy. Proc Natl Acad Sci U S A 111:1551–1556. doi:10.1073/pnas.1308963111
41. Deschepper CF, Olson JL (1985) Otis M and Gallo-Payet N (2004) Characterization of blood pressure and morphological traits in cardiovascular-related organs in 13 different inbred mouse strains. J Appl Physiol 97:369–376. doi:10.1152/japplphysiol.00073.2004
42. Barrick CJ, Rojas M, Schoonhoven R, Smyth SS, Threadgill DW (2007) Cardiac response to pressure overload in 129S1/SvImJ and C57BL/6 J mice: temporal- and background-dependent development of concentric left ventricular hypertrophy. Am J Physiol Heart Circ Physiol 292:H2119–H2130. doi:10.1152/ajpheart.00816.2006
43. Thilo F, Loddenkemper C, Berg E, Zidek W, Tepel M (2009) Increased TRPC3 expression in vascular endothelium of patients with malignant hypertension. Mod Pathol 22:426–430. doi:10.1038/modpathol.2008.200
44. Kiyonaka S, Kato K, Nishida M, Mio K, Numaga T, Sawaguchi Y, Yoshida T, Wakamori M, Mori E, Numata T, Ishii M, Takemoto H, Ojida A, Watanabe K, Uemura A, Kurose H, Morii T, Kobayashi T, Sato Y, Sato C, Hamachi I, Mori Y (2009) Selective and direct inhibition of TRPC3 channels underlies biological activities of a pyrazole compound. Proc Natl Acad Sci USA 106:5400–5405. doi:10.1073/pnas.0808793106

Supplementary Fig. 1

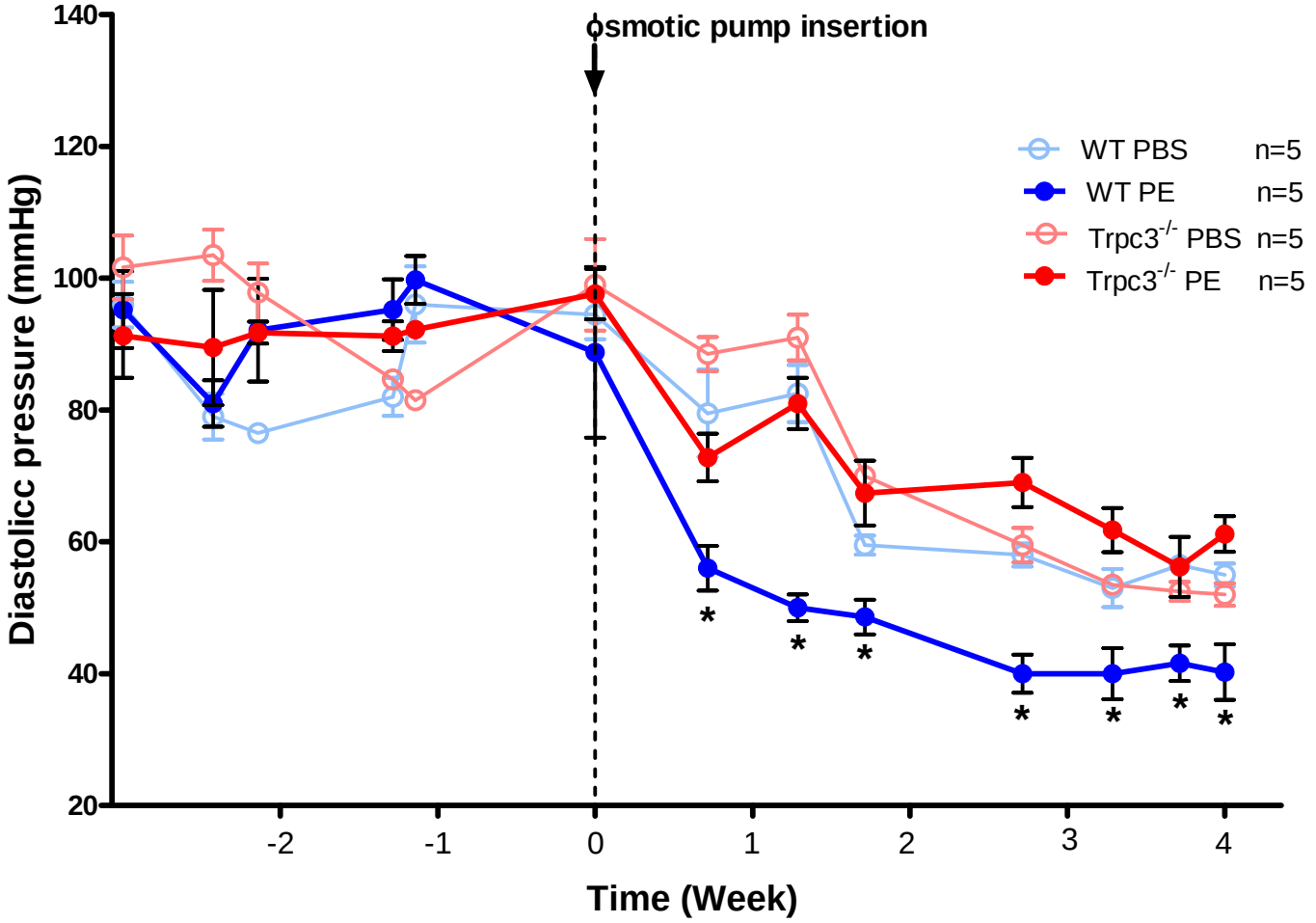

Supplementary Fig. 1 Diastolic blood pressures (BP) of WT and *Trpc3*$^{-/-}$ mice in PBS or PE infusion condition. Osmotic pump Alzet 2200 were inserted at 0 day (arrow) and PE were infused as 65 mg/kg/day. (n=7). *p<0.05 compared with PBS-infused WT.

Supplementary Fig. 2

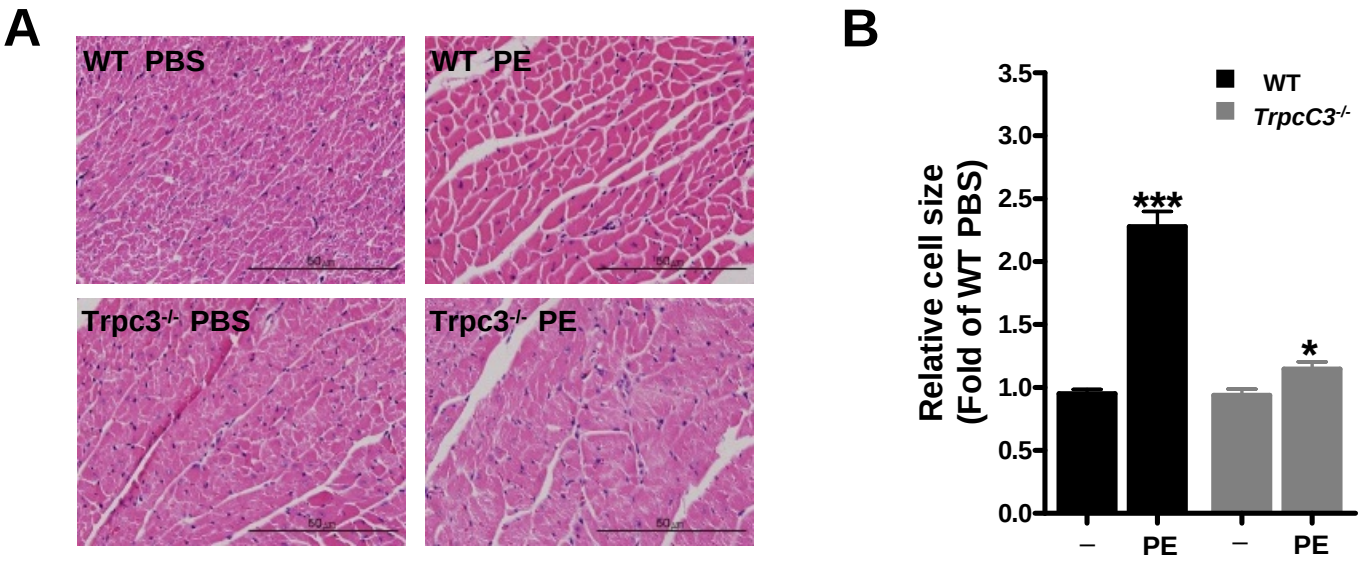

Supplementary Fig. 2 Cardio myocyte hypertrophy of PE infused WT mice. (A) Representative images showing the myocyte cell size in left ventricle of each mouse (bar, 50 μm). (B) Summary of the quantitation of relative cell size. ***p<0.0001 compared with PBS-infused WT; *p<0.05 compared with PBS-infused *Trpc3*$^{-/-}$.

Supplementary Fig. 3

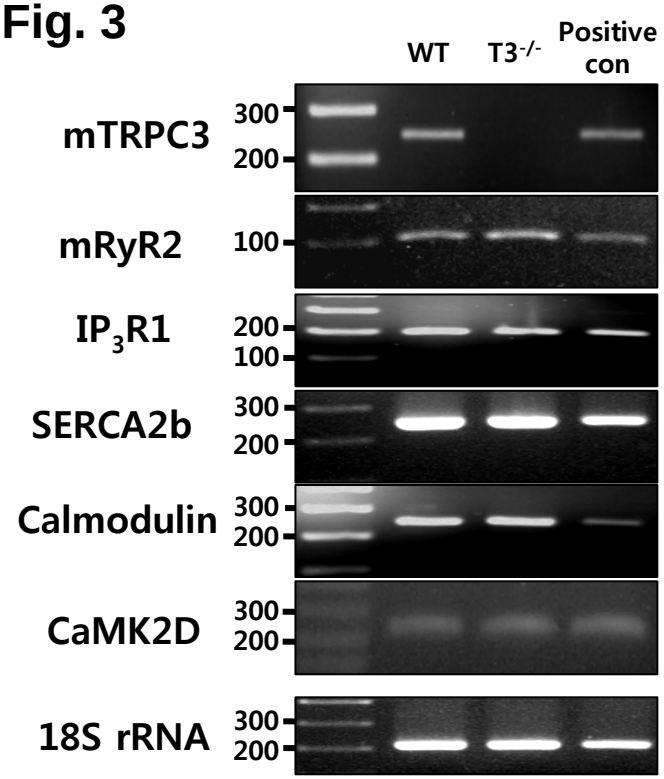

Supplementary Fig. 3 Expression of mRNAs of representative components of heart contraction was similar in WT and *Trpc3*$^{-/-}$ hearts. To determine whether reduction of $Ca_V1.2$ expression altered expression levels of other components of heart contraction, RT-PCR analysis of WT and *Trpc3*$^{-/-}$ hearts was carried out using the indicated primers, and generating products of the indicated size.

mTrpc3 forward, 5'- TCA TAC TTT ATT CTT ACT ACC TTG G-3'; reverse, 5'- ATC TCT TGG TAT GAG CTA TTA ATC-3'; 244 bp

mRyR2 forward, 5'- CTT CGA TGT TGG CCT TCA AGA G-3'; reverse, 5'- CCA ACA CGC ACT TTT TCT CCT T-3'; 100 bp

mIP3R1 forward, 5'-GAA GCA GCA TGT GTT CCT GA-3'; reverse, 5'-GGT CTA CCT CTG CAG CCA AG-3': 198 bp

mSERCA2b forward, 5'-CTG TGG AGA CCC TTG GTT GT-3'; reverse, 5'-CAG AGC ACA GAT GGT GGC TA-3'; 245 bp

mCalmodulin forward, 5'-TTG CCG TCT ATG ACC ACG TA-3'; reverse, 5'-TGC TTT TGC CAT ACA CAG TG-3'; 233 bp

mCAMK2D forward, 5'-AAG CAC CCC AAT ATT GTG AG-3'; reverse, 5'-CAA ATT CTC AGG CTT CAG GT-3'; 222 bp

18S rRNA forward, 5'-GTGGAGCGATTTGTCTGGTT-3'; reverse, 5'-CGCTGAGCCAGTCAGTGTAG-3'; 200 bp)